Catalysis Science & Technology

Accepted Manuscript

This article can be cited before page numbers have been issued, to do this please use: D. O. Aldosari, S. Iqbal, P. Miedziak, G. Brett, D. Jones, X. Liu, J. Edwards, D. Morgan, D. W. Knight and G. Hutchings, *Catal. Sci. Technol.*, 2015, DOI: 10.1039/C5CY01650A.

ROYAL SOCIETY OF CHEMISTRY

www.rsc.org/catalysis

View Article Online
DOI: 10.1039/C5CY01650A

Pd-Ru/TiO_2 catalyst – an active and selective catalyst for furfural hydrogenation

Obaid F. Aldosari, Sarwat Iqbal, Peter J. Miedziak, Gemma L. Brett, Daniel R. Jones, Xi Liu, Jennifer K. Edwards, David J. Morgan, David K. Knight, and Graham J. Hutchings*

*hutch@cardiff.ac.uk

Cardiff Catalysis Institute, Main Building Park Place, Cardiff, UK, CF10 3AT

View Article Online
DOI: 10.1039/C5CY01650A

Abstract

The selective hydrogenation of furfural at ambient temperature has been investigated using a Pd/TiO_2 catalyst. The effect of the solvent was studied and high activity and selectivity to 2-methylfuran and furfuryl alcohol was observed using octane as solvent but a number of byproducts were observed. The addition of Ru to the $PdTiO_2$ catalyst decreased the catalytic activity but improved the selectivity towards 2-methylfuran and furfuryl alcohol with decreased byproduct formation. Variation of the Ru/Pd ratio has shown an interesting effect on the selectivity. The addition of a small amount of Ru (1 wt. %) shifted the selectivity towards furfuryl alcohol and 2-methylrofuran. Further increasing the Ru ratio decreased the catalytic activity and also showed a very poor selectivity to 2-methylfuran.

Key words: Furfural, Pd/Ru catalysts, room temperature, 2-methylfuyran, furfuryl alcohol, hydrogenation, alternative fuel derivatives

View Article Online
DOI: 10.1039/C5CY01650A

Introduction

Biomass is considered as one of the most important resources of renewable energy, yet the development of efficient technologies which can utilize biomass represents a major challenge.[1] The utilization of chemical intermediates like furfural (FFR), furfuryl alcohol (FA), together with attractive biofuels like 2-methylfuran (2-MF) and 2-methyltetrahydrofuran (2-MTHF) is the main focus of much current research.[2-4] FFR, a product from xylose conversion is an important bio-derivative.[1] It is considered to be a platform chemical for the upgrading of fuels through the formation of FA and 2-MF by hydrogenation.[5] FA and 2-MF have a range of applications in the chemical industry; FA is mainly used in the manufacturing of resins,[6] and as a starting material for the synthesis of 1,5-pentanediol,[7, 8] 2-MF[9] and tetrahydrofurfuryl alcohol (THFA).[10] 2-MF is obtained from the hydrogenation of FFR and FA. The main applications of 2-MF are in the synthesis of perfume intermediates, and chloroquine lateral chains in medical applications.

Copper-based catalysts have received considerable attention for the hydrogenation of FFR. Dongxia *et al.* have reported FFR hydrogenation in the liquid phase at a temperature of 180 °C and 69-104 barg pressure of pure hydrogen with the utilization of a copper chromite catalyst.[11] The catalyst was found to be very active for the synthesis of 2-FA. Copper in combination with other metals supported on oxides e.g., Cu/Cr,[12] Cu/Fe,[13, 14] Cu/Zn/Al,[15] Cu/TiO_2,[5] Cu/SiO_2,[16-18] Cu/Ni/Mg/Al,[19] Cu/Pd,[20, 21] has been reported to be active for the hydrogenation of FFR forming 2-MF, 2-MTHF, and 2-FA. A number of other metal oxide catalysts have also been studied and found to be suitable candidates for this reaction. e.g., Ru,[22, 23] Ni,[24] Fe,[24-26] supported catalysts. Almost all of these studies have been performed under very harsh reaction conditions, both in terms of the temperature and the hydrogen pressure required to observe activity. Therefore, a process for the selective synthesis of 2-MF and 2-FA from FFR under milder reaction conditions is highly desirable. We have recently reported that Pd/TiO_2[9] and $Pd/Sn/TiO_2$[10] catalysts can be used very effectively for the conversion of FA into 2-methyfuran at room temperature. Medlin *et al.* have recently reported an application of self-assembled layers used to block the Pd active sites which can minimize the decarbonylation reaction and the corresponding side product formation during furfural hydrogenation.[27]In the present study we report the hydrogenation of FFR using the previously reported Pd/TiO_2 catalyst in 1,2-dichloroethane, toluene, methanol and octane. Variation of the solvent has shown an interesting effect on the selectivity pattern. Furthermore, we have studied the addition of a second metal component, namely Ru, and

View Article Online
DOI: 10.1039/C5CY01650A

observed lower catalytic activity, but high selectivity to 2-MF and FA with less byproduct formation compared to the unmodified Pd/TiO_2 catalysts.

Experimental

Materials

FFR (98%), 1,2-dichloroethane (98%), methanol (99.8%), octane (98%), toluene (99%) and all reaction intermediates were purchased from Sigma Aldrich and used as received. Palladium (II) chloride and ruthenium (III) chloride metal precursors were also purchased from Sigma Aldrich. TiO_2 was purchased from Degussa (P25). Pure hydrogen (99.9%) and nitrogen (99.9%) were obtained from BOC.

Catalyst preparation

All the monometallic catalysts supported on TiO_2 were prepared by a standard wet impregnation method reported previously.[10] In a typical synthesis the $PdCl_2$ was added to 2ml deionised water and stirred for approximately 15 min at 80 °C until the Pd dissolved completely. The TiO_2 support was added to the solution and stirred to form a paste. The paste was subsequently dried at 110 °C for 16 h, and calcined in static air (400 °C, 3 h, 20 $^{o}C\ min^{-1}$).

Bimetallic catalysts were prepared in the same manner, with the concomitant heating and stirring of the $PdCl_2$ and $RuCl_3$ precursors together.

Characterization

X-ray diffraction (XRD). Powder XRD was carried out using a PANalytical X'Pert Pro with a CuK_α X-ray source run at 40 kV and 40 mA fitted with an X'Celerator detector. Each sample was scanned from $2\theta = 10$ to 80 for 30 min. The catalysts were ground into fine powder form and loaded on a silicon wafer. The results obtained were compared with the information in ICDD library for each catalyst.

Temperature programmed reduction (TPR). Temperature programmed reduction/ oxidation was carried out using a TPDRO 1100 series analyser. Samples (80 mg) were pre-treated for 1 h at 130 °C (20 °C/ min) in a flow of Argon (20 mL/ min). Following this the gas flow was changed to 10% H_2/Ar or 10%O_2/He and the temperature was ramped to 800 °C

View Article Online
DOI: 10.1039/C5CY01650A

(10 °C/ min) with a 5 min hold at the T_{max}. H_2/O_2 uptake was monitored using a TCD detector.

X-ray photoelectron spectroscopy (XPS). Samples were characterized using a Kratos Axis Ultra-DLD photoelectron spectrometer, using monochromatic Al K_α radiation, at 144 W (12 mA × 12 kV) power. High resolution and survey scans were performed at pass energies of 40 and 160 eV respectively. Spectra were calibrated to the C (1s) signal for adventitious carbon at 284.8 eV and quantified using CasaXPS v2.3.17, utilizing sensitivity factors supplied by the manufacturer.

Transmission electron microscopy (TEM). TEM was carried out using a Jeol 2100 with a LaB_6 filament operating at 200 kV. Samples were prepared by dispersing the powder catalyst in ethanol and dropping the suspension onto a lacey carbon film over a 300 mesh copper grid.

FFR hydrogenation reaction.

The hydrogenation of FFR was carried out using a stainless steel stirred autoclave (50 ml, Parr Instruments, Model 5500HP) equipped with a Teflon liner using catalyst (0.1 g), FFR (1 g) and solvent (15 ml). The sealed autoclave was purged three times with N_2, and three times with H_2 before being pressurized to 3 barg with H_2. The autoclave was stirred at 1000 rpm at ambient temperature. When the reaction was completed, the mixture was cooled, filtered and the post-reaction mixture was centrifuged prior to being analysed by GC (Bruker Sion 456-GC fitted with a Br-1ms capillary column). Products were identified by comparison with the authentic samples. For the quantification of the amounts of reactant consumed and products generated an external calibration method was used, with 1-propanol being the external standard.

Results and Discussion

In our initial experiments we investigated a range of organic solvents with the 5%Pd/TiO_2 catalyst to study the hydrogenation of FFR under mild reaction conditions (25 °C and 3 barg H_2). The products expected from the hydrogenation of FFR that can be used as fuel derivatives are summarized in scheme 1.

The main target products we focused on in this study are 2-MF, and FA. Table 1 shows the comparison of various organic solvents for the catalyzed reactions. Generally the solvent is chosen in order to increase the concentration of dissolved hydrogen, and as a result

View Article Online
DOI: 10.1039/C5CY01650A

enables an increase in the reaction rate.[28] We have observed a high catalytic activity with toluene and methanol but the selectivity observed was completely different between the two solvents. The reaction in toluene showed a high selectivity of 2-MF and THFA. The use of methanol as the solvent led to a significantly increased selectivity of THFA alcohol along with a large amount of side products. Formation of THFA requires the selective hydrogenation of the furan double bonds with the hydrogenation of the alcohol so it follows a different reaction pathway, as shown in scheme 1.

The reaction in 1,2-dicholoroethane showed formation of a mixture of products and a very small amount of the desirable products were produced, which is in contrast to our previous observations on the hydrogenation of FA where we achieved a full conversion of FA into 2-MF in 1,2-dichloroethane.[9]

Although, the catalytic activity was far higher with methanol, 1,2-dichloroethane and toluene but the amount of side products was also very high; therefore we chose octane for further investigation of the reaction parameters. Interestingly, the selectivity observed with octane was shifted more towards 2-MF and FA with far lower amounts of side products (mainly acetals and ketals) compared with the other solvents.

To further probe the reaction we varied the loading of the Pd from 1 to 5 wt% and the data for FFR hydrogenation is provided in Table 2. Initially we performed the blank reactions as well as reactions with the pure TiO_2 and observed no activity. Increasing the loading of Pd metal from 1% to 5% increased the catalytic activity, although not proportionally, and also increased the selectivity of 2-MF significantly.

We have previously reported the characterization of all these catalysts with the variation of Pd metal loading.[9] The particle size of Pd was found to be very low (<2nm) and there was no major difference observed in the particle size distribution when the metal loading was increased from 1% to 5% wt. Given the uniformity of the particle size distribution we can link the increased catalytic activity to an increased concentration of active metal sites.

A time on line study for FFR hydrogenation was performed using 5% Pd/TiO_2 catalyst and the activity data is provided in Figure 1. As expected there was an increase in conversion with an increase in the reaction time from 30 min to 180 min. In the initial 30 min only 2-MF and FA were formed with no side products being observed, an increase in the amount of byproducts was observed, however, when the reaction was performed over longer times. Small amounts of THFA were also observed which could be a hydrogenation product

View Article Online
DOI: 10.1039/C5CY01650A

of FFR or FA. It is possible for side reactions from FA and 2-MF to occur as shown in scheme 1, which can further react to form various other molecules like acetals and ketals.

From the data in Figure 1 it is apparent that the monometallic 5%Pd/TiO_2 catalyst displays high activity for FFR hydrogenation and the selectivity of 2-MF and FA was high but there was still a significant number of side products. We have previously shown that the addition of a second metal (Sn) into Pd/TiO_2 catalyst can improve the selectivity pattern in FA hydrogenation[10] and changing the ratio of metals in a bimetallic catalyst can have a significant effect on the reaction profile in benzyl alcohol and hexenol oxidation reactions.[29, 30] Ru is one of the most studied metals for the hydrogenation reactions of furan-derived compounds,[31-35] therefore, we synthesized bimetallic catalysts with the different ratios of Ru and Pd. The catalysts were tested for FFR hydrogenation reaction in octane at room temperature under 3 barg pressure of hydrogen. The data is presented in Table 3.

Monometallic 5%Ru/TiO_2 catalysts whilst exhibiting a lower catalytic activity produced exclusively FA. The addition of a small amount of Pd showed a decrease in selectivity towards FA and the formation of 2-MF was obvious.

Furthermore increasing the Pd content, whilst maintaining an overall 5 wt% metal loading, served to increase the catalytic activity and improved the selectivity towards FA compared with 2-MF. When both metals were present in a 1:1 ratio the conversion was high and FA was the dominant product and lower amounts of 2-MF (also a consecutive product of FA) were observed. Interestingly, much lower amounts of side products was observed with the 1% Ru-4% Pd/TiO_2 catalyst. This catalyst showed the highest selectivity to 2-MF and FA compared with the pure monometallic 5%Ru/TiO_2 and 5%Ru/TiO_2 catalysts. The small amount of ruthenium metal may have prevented the side reaction pathways, allowing the consecutive hydrogenation reaction to take place. Further increasing the amount of Pd from 4% to 4.5% showed no particular change in activity or selectivity to 2-MF but the number of side products increased from 2 to 7%. From these data we conclude that the addition of 1% Ru into Pd/TiO_2 is optimal composition required for the synthesis of 2-MF and FA from FFR under these reaction conditions. Luo *et al.* have reported the use of palladium ruthenium alloyed catalysts for the hydrogenation, suggesting that the palladium dilutes and separates the active ruthenium sites,[36] it is possible that we are observing a similar effect for this case, however, for this reaction the palladium is the active species being diluted and isolated by the ruthenium.

Powder X-ray diffraction (XRD) patterns of monometallic unreduced Ru/TiO_2, Pd/TiO_2 and Ru/Pd/TiO_2 catalysts are shown in Figure 2. There was no significant difference

View Article Online
DOI: 10.1039/C5CY01650A

observed between these catalysts and the major component reflections were related with titania (P25). We have used a mixture of anatase and rutile titania and both of these phases remained stable. It suggested that either the particle size of Pd and Ru particles (metallic or oxide) was too small to be detected by XRD or the metals were homogeneously dispersed on the surface of TiO_2.

To try to explain the differences observed in the catalytic performance for the catalysts we analyzed them using TEM, and the representative images are shown in Figure 3 and the associated particle size distributions are shown in Figure 4. The most active catalyst was the 5%Pd/TiO_2 and we have previously reported the characterization of this catalyst[9], it had an average particle size of 1.1nm. The catalysts in general seem to have lower activity as the ratio of palladium/ruthenium decreased. The 0.5%Ru:4.5%Pd/TiO_2 and 1%Ru:4%Pd/TiO_2 catalysts display identical conversions (39%), the TEM analysis of these catalysts reveals that they also have a very small average particle sizes of 1.3 and 1.1 nm respectively (Figures 3/4e and f). This is slightly larger than those reported for the 5%Pd/TiO_2 catalyst. This suggests that there is an inverse relationship between the activity and the particle size for this reaction system. There are, however, significant differences in the selectivity of the two catalysts which suggests the reaction pathways are more related to the composition of the catalysts than the particle size.

2%Ru:3%Pd/TiO_2 has a slightly lower activity than that would be expected from the pattern observed for the other catalysts. The TEM images and PSD are shown in Figure 3d. The average particle size for this catalyst is larger than those with the lower amounts of palladium at 2 nm, Figure 4d shows that the particles seem to be larger with some evidence of clusters forming, interestingly the 2.5%Ru-2.5%Pd/TiO_2 catalyst (Figure 3c) has a smaller average particle size, with some evidence of slightly larger particles seen but not as many as the 2%Ru-3%Pd/TiO_2 catalyst. Again this may correlate directly with the conversion data with the 2.5%Ru-2.5%Pd/TiO_2 catalysts slightly more active than the 2%Ru:3%Pd/TiO_2 catalyst.

The catalysts with the lowest amount of palladium, 3%Ru-2%Pd/TiO_2 and 4%Ru-1%Pd/TiO_2 (Figures 3b and 3a respectively), once again have a smaller particle size, however, the activity of these catalysts is lower, suggesting that at low palladium content the particle size is not the only factor that affects the activity. As the most active catalyst was the palladium monometallic catalyst and the ruthenium monometallic catalyst was amongst the least active catalyst it seems likely that the palladium is the active component in these catalysts, we suggest that when the relative amount of ruthenium in the catalyst becomes too

View Article Online
DOI: 10.1039/C5CY01650A

large the catalysts loses activity as the substrate can no longer access the active palladium sites. Interestingly the 3%Ru-2%Pd/TiO_2 catalyst has the smallest particle size of all the catalysts studied in this work and also has a conversion that is relatively higher than would be expected if the activity was solely related to the palladium content. Overall the TEM suggests that to form an active catalyst for this reaction small particle are required, however a significant amount of the metal component must be palladium but the amount of ruthenium can be tuned to affect the reaction selectivity.

TPR measurements were performed with all the catalysts in order to investigate the reducibility of metal oxide species. A combined TPR profile is presented in Figure 5. Monometallic 5% Ru/TiO_2 catalyst (a) showed a reduction peak above 150 °C which became broader with an addition of Pd (b-e). On the other hand the monometallic 5% Pd/TiO_2 (h) catalyst showed a reduction peak at a temperature less than 100 °C. The catalysts with 1%Ru/4% Pd (f) and 0.5% Ru/4.5% Pd (g) showed a very different reduction behavior compared with the other bimetallic catalysts. A feature was observed around 100 °C in both of these catalysts which can be related to the emission of trapped hydrogen (Pd β hydride species) above 90 °C. This feature of hydrogen evolution indicates that hydrogen can be adsorbed on the surface of the catalyst at sub ambient temperatures and gets released in the form of hydrogen molecules when the temperature is raised above 90 °C.[37] To further probe the nature of the metal particles we performed CO chemisorption studies with these catalysts and normalized the metal surface area with the activity. We observed that the specific activity was not a function of the metal surface area. As expected, the Pd dispersion increased with an increase in the concentration of Pd.

XPS analysis of mono and bimetallic unreduced catalysts are presented in Figure 6. It revealed multiple oxidation states for both Pd and Ru. For monometallic 5% Pd, the spectra was dominated by a signal at 337.7 eV attributable to Pd-Cl bonds with a ratio of *ca.* 1:1 and supported by the significant residual chlorine at 198.4 eV which is characteristic of metal-chlorine bonds and as observed for Pd deposited from solution on Fe_3O_4.[38] Additionally, PdO was also evident at 336 eV. In contrast, the monometallic ruthenium catalyst was found to be chloride free, but exhibited two species with binding energies of 280.1 and 280.8 eV attributable to Ru(0) [39]and RuO_2 respectively[40] in a 1:1 ratio suggesting the metallic ruthenium was covered by an oxide layer. The presence of RuO_2 was also supported by the O(1s) shoulder ca. 529 eV consistent with the RuO_2.

View Article Online
DOI: 10.1039/C5CY01650A

For the bimetallic catalysts, the two Ru oxidation states remain, although for the 3%Ru-2%Pd/TiO_2 catalyst and those with a higher Pd content, there was a 0.4 shift to higher binding energy for the Ru(3d) signals and attributed to a particle size effect, however, the Ru(0)/Ru(IV) ratio remained constant at *ca.* 1:1. No shift in Pd binding energy was seen with changing the metal ratio, neither were shifts or reduced species observed in the Ti(2p) spectra as reported previously by Luo *et al* for RuPd/TiO_2 systems.[36] Instead, the Pd was present at 335.5 eV (Pd(0)) and 337.1 eV (Pd-Cl) which was different to that of the monometallic where both Pd-Cl and PdO were observed. It is worthy to note that the Pd(0) binding energy was somewhat higher than that expected for metallic Pd particles and may be attributable to (i) Pd^{2+} species formed by a charge transfer with Cl^{-1} which remains on the surface, or (ii) particle size dependent screening effects of the Pd core-hole which results in higher binding energies for the smaller particles[41-43] . Based on the microscopy (Figures 2 and 3) the latter is considered to be the case here.

Conclusions

We have reported an efficient and novel catalyst composition for the conversion of FFR into useful organic molecules (2-MF, and 2FA) at room temperature and low hydrogen pressure. Overall we conclude that the most effective catalyst for this reaction is the 1%Ru:4%Pd/TiO_2. This catalyst represented the best compromise of conversion of FFR and selectivity to the desired products 2-MF and FA. TEM particle size distributions of the catalysts indicated that for this reaction small metal particles are required; however, the particle size is not the only consideration when trying to optimise these catalysts. XPS suggested that the oxidation state of the ruthenium is also an important factor as when the relative amount of ruthenium in the metallic sate was increased the activity was reduced. By tuning the ratio of palladium to ruthenium we can form a catalyst where we can direct the selectivity towards the products that are useful as fuel additives under mild, green reaction conditions.

Acknowledgments

The authors would like to thank the EPSRC (EP/K014854/1) and the Research Campus at Harwell for access to the transmission electron microscope. The raw data is provided in DOI:

View Article Online
DOI: 10.1039/C5CY01650A

http://dx.doi.org/10.17035/d.2015.100119. Obaid F. Aldosari would like to thank Royal embassy of Saudi Arabia for funding his PhD.

References

1. G. W. Huber, S. Iborra and A. Corma, *Chem. Rev.* , 2006, **106**, 4044-4098.
2. J.-P. Lange, d. H. E. van, B. J. van and R. Price, *ChemSusChem*, 2012, **5**, 150-166.
3. J. G. Stevens, R. A. Bourne, M. V. Twigg and M. Poliakoff, *Angew. Chem., Int. Ed.*, 2010, **49**, 8856-8859.
4. Y. Nakagawa, M. Tamura and K. Tomishige, *ACS Catal.*, 2013, **3**, 2655-2668.
5. H. Zhang, C. Canlas, A. Jeremy Kropf, J. W. Elam, J. A. Dumesic and C. L. Marshall, *J. Catal.*, 2015, **326**, 172-181.
6. A. Corma, S. Iborra and A. Velty, *Chem Rev*, 2007, **107**, 2411-2502.
7. H. Adkins and R. Connor, *J. Am. Chem. Soc.*, 1931, **53**, 1091-1095.
8. B. Zhang, Y. Zhu, G. Ding, H. Zheng and Y. Li, *Green Chem.*, 2012, **14**, 3402-3409.
9. S. Iqbal, X. Liu, O. F. Aldosari, P. J. Miedziak, J. K. Edwards, G. L. Brett, A. Akram, G. M. King, T. E. Davies, D. J. Morgan, D. K. Knight and G. J. Hutchings, *Catal. Sci. Technol.*, 2014, **4**, 2280-2286.
10. G. M. King, S. Iqbal, P. J. Miedziak, G. L. Brett, S. A. Kondrat, B. R. Yeo, X. Liu, J. K. Edwards, D. J. Morgan, D. K. Knight and G. J. Hutchings, *ChemCatChem*, 2015, **7**, 2122-2129.
11. D. Liu, D. Zemlyanov, T. Wu, R. J. Lobo-Lapidus, J. A. Dumesic, J. T. Miller and C. L. Marshall, *J. Catal.*, 2013, **299**, 336-345.
12. J. G. M. Bremner and R. K. F. Keeys, *J. Chem. Soc.*, 1947, 1068-1080.
13. Y.-L. Zhu, H.-W. Xiang, Y.-W. Li, H. Jiao, G.-S. Wu, B. Zhong and G.-Q. Guo, *New J. Chem.*, 2003, **27**, 208-210.
14. J. Lessard, J.-F. Morin, J.-F. Wehrung, D. Magnin and E. Chornet, *Top. Catal.*, 2010, **53**, 1231-1234.
15. Y. Wang, M. Zhou, T. Wang and G. Xiao, *Catal. Lett.*, 2015, Ahead of Print.
16. D. Vargas-Hernandez, J. M. Rubio-Caballero, J. Santamaria-Gonzalez, R. Moreno-Tost, J. M. Merida-Robles, M. A. Perez-Cruz, A. Jimenez-Lopez, R. Hernandez-Huesca and P. Maireles-Torres, *J. Mol. Catal. A: Chem.*, 2014, **383-384**, 106-113.
17. M. M. Villaverde, N. M. Bertero, T. F. Garetto and A. J. Marchi, *Catal. Today*, 2013, **213**, 87-92.
18. Z. Li, G. Wang and W. Li, *Adv. Mater. Res.* , 2012, **599**, 27-31.
19. C. Xu, L. Zheng, D. Deng, J. Liu and S. Liu, *Catal. Commun.*, 2011, **12**, 996-999.
20. F. Dong, Y. Zhu, G. Ding, J. Cui, X. Li and Y. Li, *ChemSusChem*, 2015, **8**, 1534-1537.
21. K. Fulajtarova, T. Sotak, M. Hronec, I. Vavra, E. Dobrocka and M. Omastova, *Appl. Catal., A*, 2015, **502**, 78-85.
22. P. Panagiotopoulou, N. Martin and D. G. Vlachos, *ChemSusChem*, 2015, **8**, 2046-2054.
23. M. J. Gilkey, P. Panagiotopoulou, A. V. Mironenko, G. R. Jenness, D. G. Vlachos and B. Xu, *ACS Catal.*, 2015, **5**, 3988-3994.
24. S. Sitthisa, W. An and D. E. Resasco, *J. Catal.*, 2011, **284**, 90-101.
25. Z. Li, S. Kelkar, C. H. Lam, K. Luczek, J. E. Jackson, D. J. Miller and C. M. Saffron, *Electrochim. Acta*, 2012, **64**, 87-93.

View Article Online
DOI: 10.1039/C5CY01650A

26. H.-Y. Zheng, Y.-L. Zhu, B.-T. Teng, Z.-Q. Bai, C.-H. Zhang, H.-W. Xiang and Y.-W. Li, *J. Mol. Catal. A: Chem.*, 2006, **246**, 18-23.
27. S. H. Pang, C. A. Schoenbaum, D. K. Schwartz and J. W. Medlin, *ACS Catal.*, 2014, **4**, 3123-3131.
28. P. A. Tooley, C. Ovalles, S. C. Kao, D. J. Darensbourg and M. Y. Darensbourg, *J. Am. Chem. Soc.*, 1986, **108**, 5465-5470.
29. J. Pritchard, L. Kesavan, M. Piccinini, Q. He, R. Tiruvalam, N. Dimitratos, J. A. Lopez-Sanchez, A. F. Carley, J. K. Edwards, C. J. Kiely and G. J. Hutchings, *Langmuir*, 2010, **26**, 16568-16577.
30. H. Alshammari, P. J. Miedziak, D. J. Morgan, D. W. Knight and G. J. Hutchings, *Green Chem.*, 2013, **15**, 1244-1254.
31. G. R. Jenness and D. G. Vlachos, *J. Phys. Chem. C*, 2015, **119**, 5938-5945.
32. R. Herbois, S. Noel, B. Leger, S. Tilloy, S. Menuel, A. Addad, B. Martel, A. Ponchel and E. Monflier, *Green Chem.*, 2015, **17**, 2444-2454.
33. A. A. Dwiatmoko, S. Lee, H. C. Ham, J.-W. Choi, D. J. Suh and J.-M. Ha, *ACS Catal.*, 2015, **5**, 433-437.
34. R. M. Mironenko, O. B. Belskaya, T. I. Gulyaeva, A. I. Nizovskii, A. V. Kalinkin, V. I. Bukhtiyarov, A. V. Lavrenov and V. A. Likholobov, *Catal. Today*, 2015, **249**, 145-152.
35. N. S. Biradar, A. A. Hengne, S. N. Birajdar, R. Swami and C. V. Rode, *Org. Process Res. Dev.*, 2014, **18**, 1434-1442.
36. W. Luo, M. Sankar, A. M. Beale, Q. He, C. J. Kiely, P. C. A. Bruijnincx and B. M. Weckhuysen, *Nat. Commun.*, 2015, **6**, 6540.
37. U. S. Ozkan, M. W. Kumthekar and G. Karakas, *Catal. Today*, 1998, **40**, 3-14.
38. H.-F. Wang, H. Ariga, R. Dowler, M. Sterrer and H.-J. Freund, *J. Catal.*, 2012, **286**, 1-5.
39. C. Elmasides, D. I. Kondarides, W. Gruenert and X. E. Verykios, *J. Phys. Chem. B*, 1999, **103**, 5227-5239.
40. S. Iqbal, S. A. Kondrat, D. R. Jones, D. C. Schoenmakers, J. K. Edwards, L. Lu, B. R. Yeo, P. P. Wells, E. K. Gibson, D. J. Morgan, C. J. Kiely and G. J. Hutchings, *ACS Catal.*, 2015, **5**, 5047-5059.
41. M. G. Mason, *Phys. Rev. B: Condens. Matter*, 1983, **27**, 748-762.
42. G. K. Wertheim, S. B. DiCenzo and S. E. Youngquist, *Phys. Rev. Lett.*, 1983, **51**, 2310-2313.
43. F. A. Marks, I. Lindau and R. Browning, *J. Vac. Sci. Technol., A*, 1990, **8**, 3437-3442.

View Article Online
DOI: 10.1039/C5CY01650A

Tables and figures

Table *1*. Effect of solvents on FFR hydrogenation with 5%Pd/TiO_2

Solvents	Conversion (%)	Product selectivity (%)				
		2-MF	FA	THFA	2-MTHF	Others*
1,2-dichloroethane	100	2.5	0	9	3.7	84.7
Toluene	98	42.8	4.1	10.3	0.6	42.3
Methanol	92.2	0	0	26.9	4.8	68
Octane	65.4	36.2	35.6	4.8	0	22

Reaction conditions: RT, 3 barg H_2, 5%Pd/TiO_2 catalyst (0.1g), FFR (1g), solvent (15ml), 120 min.

*Acetals, ketals and polymeric species

View Article Online
DOI: 10.1039/C5CY01650A

Table *2*. Effect of Pd metal loading on FFR hydrogenation

Catalysts	Conversion (%)	Product selectivity (%)			
		2-MF	FA	THFA	Others*
1% Pd/TiO_2	20.7	7.0	73	14	6.0
2.5% Pd/TiO_2	53.2	20	40	7.0	33
5% Pd/TiO_2	65	38	35	5	22

Reaction conditions: RT, 3 barg H_2, catalyst (0.1g), FFR (1g), octane (15ml), 120min.

*Acetals, ketals and polymers

View Article Online
DOI: 10.1039/C5CY01650A

Table *3*. Effect of addition of Ru into Pd/TiO_2 catalyst

Catalysts	Conversion (%)	**Product selectivity (%)**				
		2-MF	FA	THFA	Others*	TOF(10^{-2})
$5\%Ru/TiO_2$	8.2	0	100	0		4.1
4%Ru-1%Pd/TiO_2	5	9.2	83.8	0	6.8	2.5
3%Ru-2%Pd/TiO_2	21.5	15.1	67.9	0	17.1	1.0
2.5%Ru-2.5%Pd/TiO_2	33.8	14	58	0.4	27.6	1.6
2%Ru-3%Pd/TiO_2	30	8.7	65.8	0	23.8	1.5
1%Ru-4%Pd/TiO_2	39.3	51.5	45.3	1.1	2.1	1.9
0.5%Ru-4.5%Pd/TiO_2	39.2	50.8	39.8	1.8	7.6	1.6
$5\%Pd/TiO_2$	65.4	36.2	28.6	4.8	30.4	3.2

Reaction conditions: RT, 3 barg H_2, catalyst (0.1g), FFR (1g), octane (15ml), 120min.

*Acetals, ketals and polymers

View Article Online
DOI: 10.1039/C5CY01650A

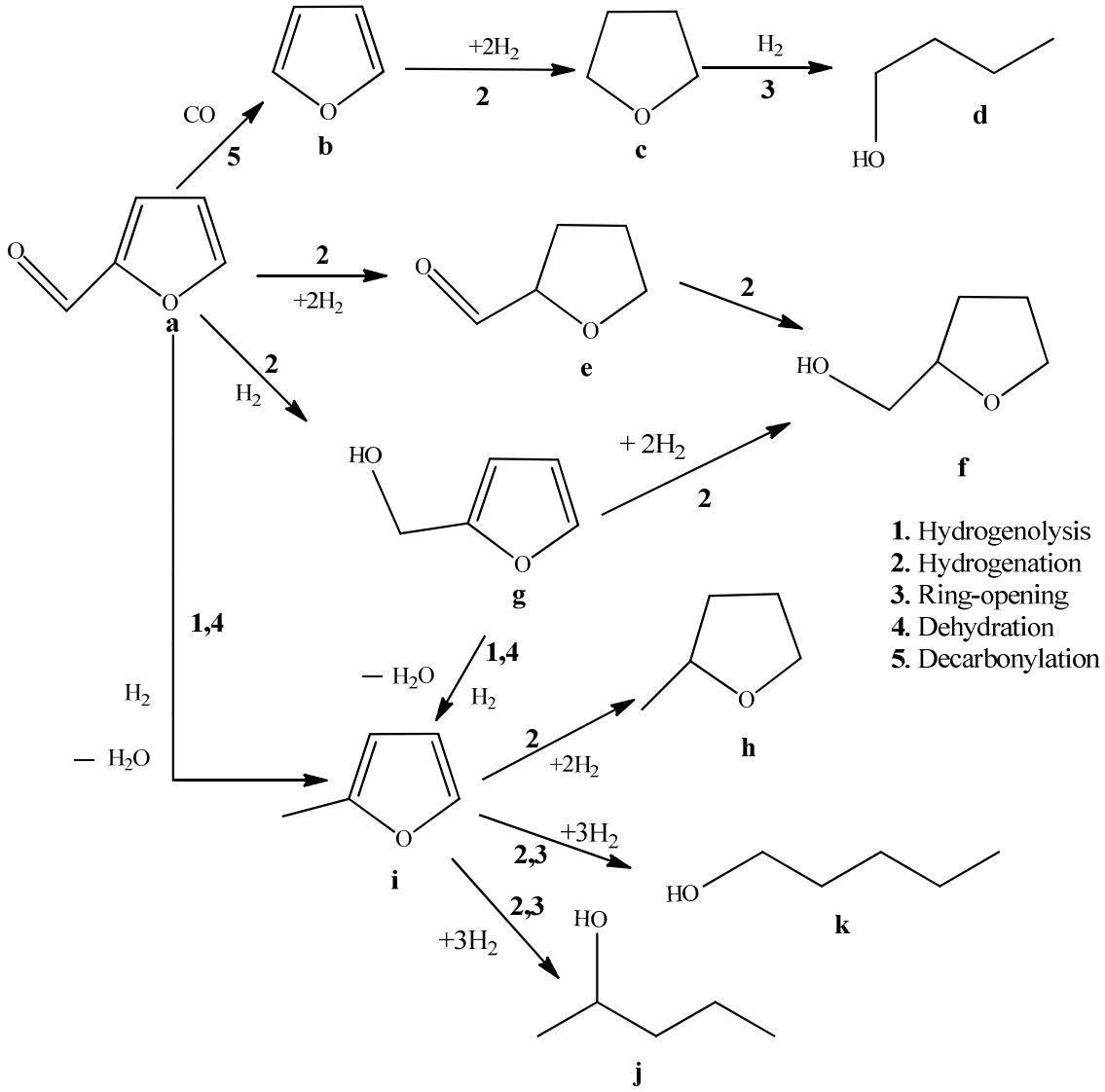

Scheme *1*. Reaction pathways for FFR hydrogenation. *Key*: **a**. Furfural (FFR), **b**. Furan (F), **c**. Tetrahydrofuran (THF), **d**. Butanol (BuOH), **e**. Tetrahydrofurfural (THFF), **f**. Tetrahydrofurfuryl alcohol (THFA), **g**. Furfuryl alcohol (FA), **h**. 2-Methyltetrahydrofuran (2-MTHF), **i**. 2-Methylfuran (2-MF), **j**. 2-Pentanol (2-PeOH), **k**. 1-Pentanol (1-PeOH).

View Article Online
DOI: 10.1039/C5CY01650A

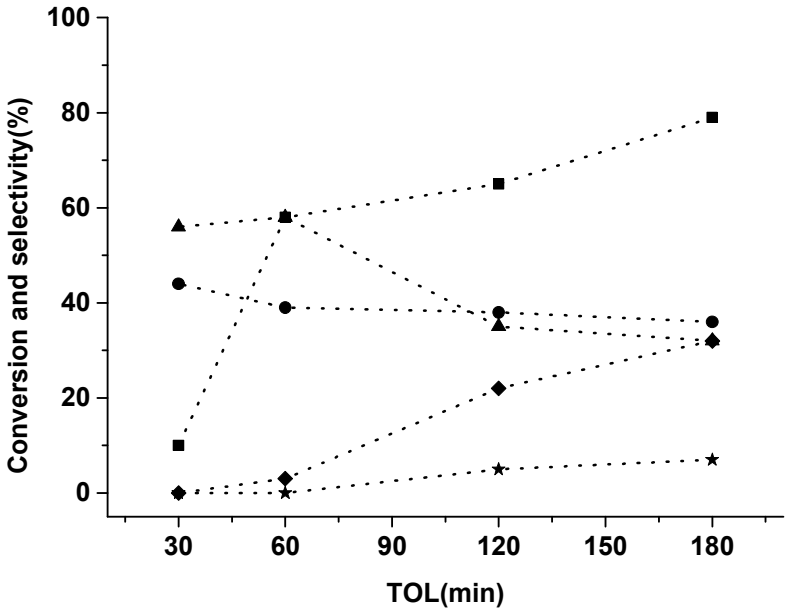

Figure *1*. Time online data for FFR hydrogenation with 5% Pd/TiO_2 catalyst. *Key*: ■ Conversion, ● 2-MF, ▲ FA, ♦ THFA, ★ Other minor products

View Article Online
DOI: 10.1039/C5CY01650A

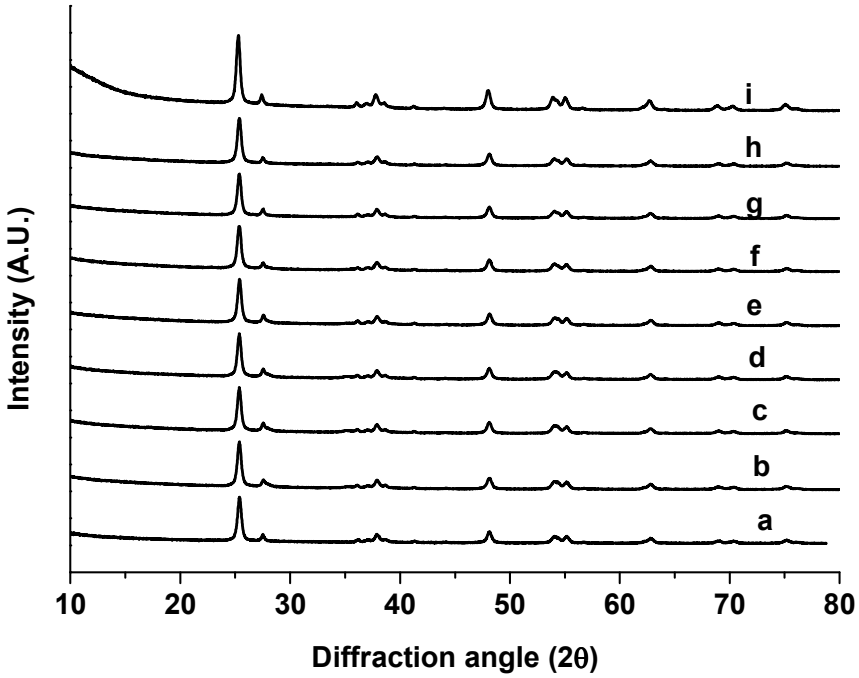

Figure *2*: XRD patterns of (a) TiO_2 P25 (b) 5%Ru/TiO_2 (c) 4%Ru-1%Pd/TiO_2, (d) 3%Ru-2%Pd/TiO_2, (e) 2.5%Ru-2.5%Pd/TiO_2, (f) 2%Ru-3%Pd/TiO_2, (g) 1%Ru-4%Pd/TiO_2, (h) 0.5%Ru-4.5%Pd/TiO_2, (i) 5%Pd/TiO_2.

View Article Online
DOI: 10.1039/C5CY01650A

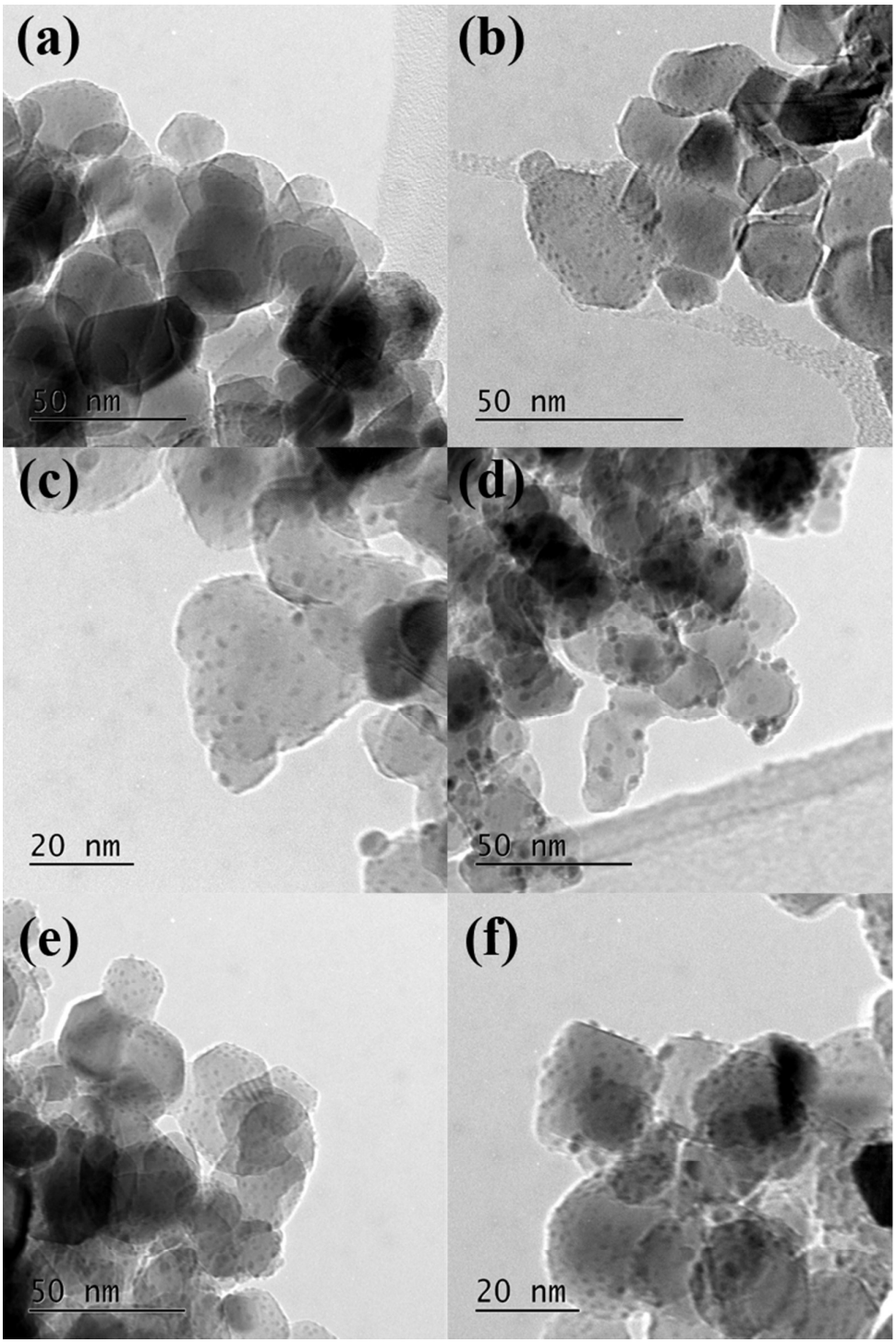

Figure ***3:*** TEM images of a) 4%Ru-1%Pd/TiO_2; b) 3%Ru-2%Pd/TiO_2; c) 2.5%Ru-2.5%Pd/TiO_2, d) 2%Ru-3%Pd/TiO_2; e) 1%Ru4%Pd/TiO_2 and f) 0.5%Ru-4.5%Pd/TiO_2.

View Article Online
DOI: 10.1039/C5CY01650A

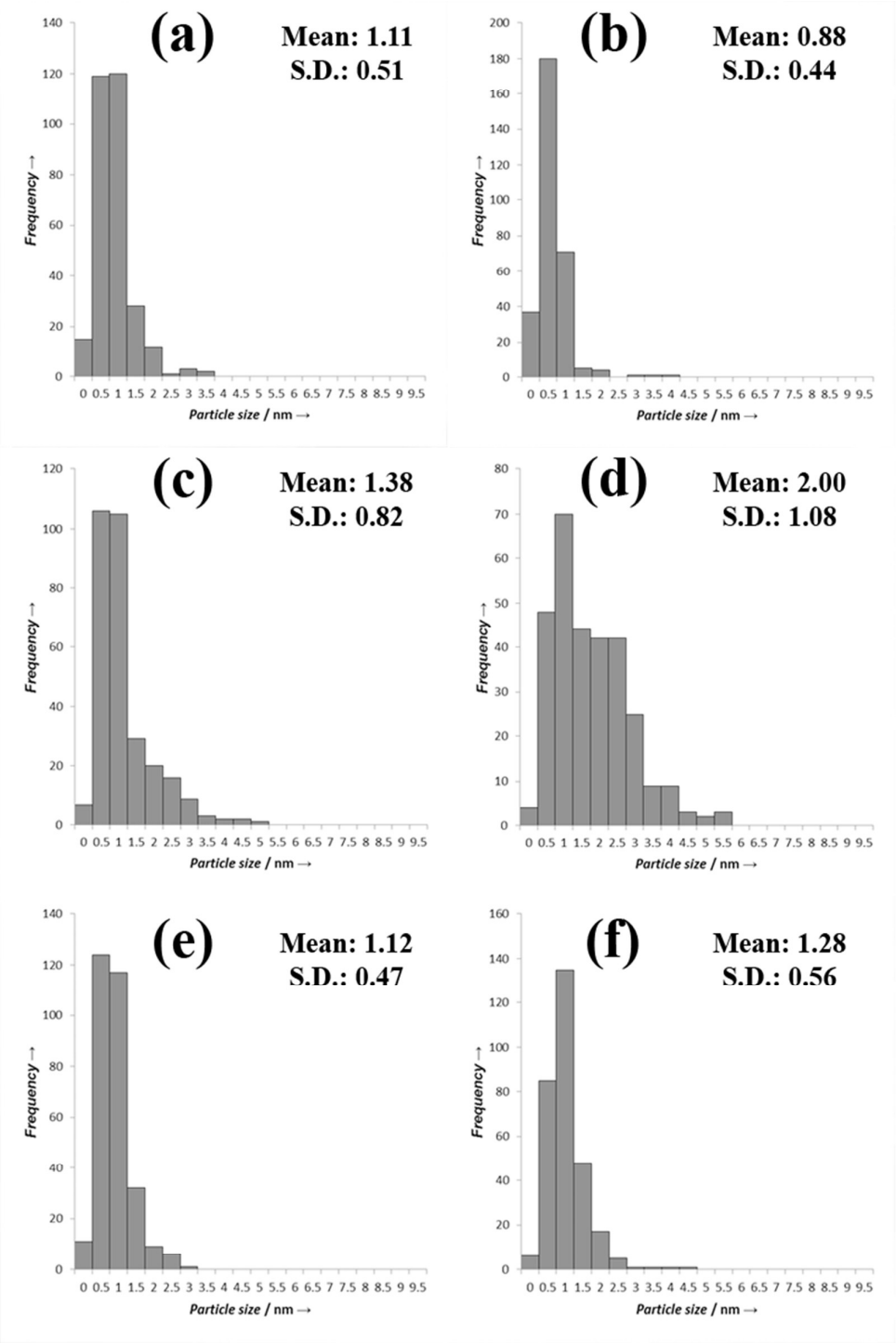

Figure *4:* TEM PSDs a) 4%Ru-1%Pd/TiO_2; b) 3%Ru-2%Pd/TiO_2; c) 2.5%Ru-2.5%Pd/TiO_2, d) 2%Ru-3%Pd/TiO_2; e) 1%Ru4%Pd/TiO_2 and f) 0.5%Ru-4.5%Pd/TiO_2.

View Article Online
DOI: 10.1039/C5CY01650A

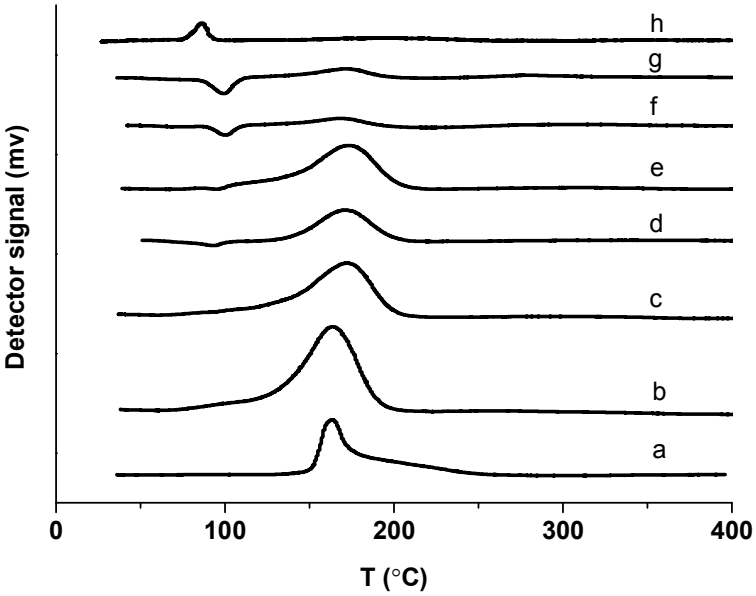

Figure *5*: TPR profile of (a) 5%Ru/TiO_2, (b) 4%Ru-1%Pd/TiO_2, (c) 3%Ru-2%Pd/TiO_2, (d) 2.5%Ru-2.5%Pd/TiO_2, (e) 2%Ru-3%Pd/TiO_2, (f) 1%Ru-4%Pd/TiO_2, (g) 0.5%Ru-(h) 4.5%Pd/TiO_2, 5%Pd/TiO_2.

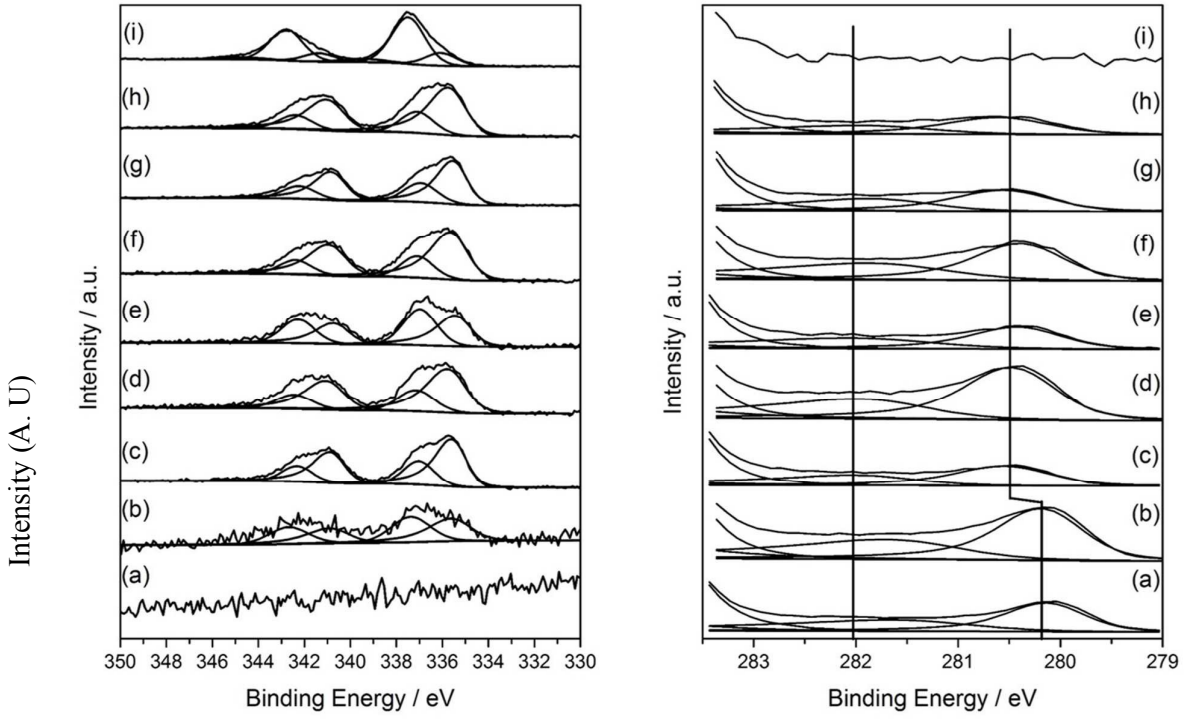

Figure *6*: XPS profiles of Pd(3d) and Ru(3d) core-level spectra of TiO_2 supported Pd with different Pd:Ru ratios. (a) 5%Ru/TiO_2, (b) 4%Ru-1%Pd/TiO_2, (c) 3%Ru-2%Pd/TiO_2, (d)

View Article Online
DOI: 10.1039/C5CY01650A

2.5%Ru-2.5%Pd/TiO_2, (e) 2%Ru-3%Pd/TiO_2, (f) 1%Ru-4%Pd/TiO_2, (g) 0.5%Ru-4.5%Pd/TiO_2, (h) 5%Pd/TiO_2, (i) 5% Pd/TiO_2 .

View Article Online
DOI: 10.1039/C5CY01650A

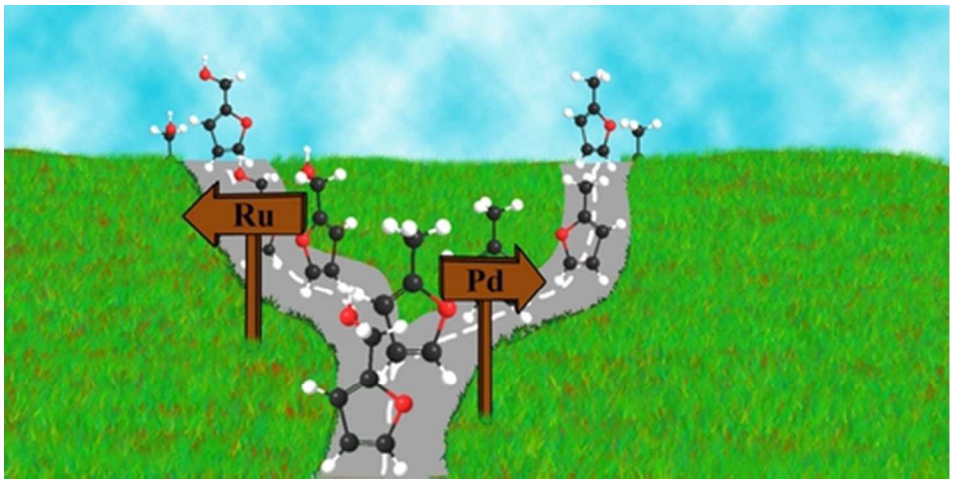

Graphical abstract
39x19mm (300 x 300 DPI)